Arab J Geosci
DOI 10.1007/s12517-011-0502-5

ORIGINAL PAPER

Salinisation origin and hydrogeochemical behaviour of the Djerid oasis water table aquifer (southern Tunisia)

Samir Kamel

Received: 26 August 2011 / Accepted: 2 December 2011

Abstract The shallow Plio-Quaternary (PQ) water table, present over almost the whole Djerid and Chott El Gharsa basins (southern Tunisia), is used as a complement of oases irrigation, especially in summer season. The simplicity of the Plio-Quaternary lithology is confronted to the complexity of the mineralisation mechanisms and the water origin in this aquifer. An approach combining the use of water-dissolved chemical species and isotopic contents has been used to better understand the PQ behaviour under severe increasing exploitation and to determinate the origin of its different water bodies. In southern Tunisia, the aquifer system is composed of the upper unconfined PQ aquifer, the intermediate semi-confined/confined Complexe Terminal (CT) and the deeper confined Continental Intercalaire (CI). Chemical analyses highlighted an origin of mineralisation in close relationship to the dissolution of both sulphated salts ($MgSO_4$ and Na_2SO_4) and chlorinated salts (NaCl and MgCl) abundant in the surface and subsurface gypsum crust. Positive correlations between gypsum anhydrite, mirabilite, thenardite and halite saturation indexes with respective mineral species, confirm evaporites dissolutions. Isotopic data showed that in addition of sporadic rainfall events, there is a contribution from the CI and the CT Saharan groundwaters, recharging the PQ aquifer in the study area. Return flow irrigation is partly affected by evaporation, before recharging the shallow aquifer, in oases limits.

Keywords Oases · Water table aquifer · Evaporation · Dissolution · Crust · Vertical leakage · Stable isotopes · Tunisia

S. Kamel (✉)
Institut Supérieur des Sciences et Techniques des Eaux de Gabès,
Cité Erriadh, Campus Universitaire,
Zrig, Gabès 6072, Tunisia
e-mail: Samir.Kamel@isstegb.rnu.tn

Introduction

At the beginning, the oases have been created around the artesian springs, forming assembly points of desert nomads. Based on landform, oases, in southern Tunisia, can be classified as alluvial plain (Chott Djerid and Chott el Gharsa margins), mountains (Metlaoui-Gafsa and Northern Chotts range piedmonts) and coastal (around Gulf of Gabes) (Coque 1962).

Saharan hot strong winds and sands, serious soil salinisation and water insufficiency are the natural causes for the disappearance of some ancient oases (Mamou and Kassah 2002).

The study area is located in southwestern Tunisia between longitude 7°30′–8°30′ east and latitude 33°30′–34°30′ north. It is limited in the west by the Algerian frontier, in the north by the Metlaoui Chain, in the east by the gulf of Gabes and in the south by the Chott Djerid depression (Fig. 1). The study area is famous in Tunisia for production dates and known as the "Djerid" region.

The development and evolution of oases is mainly decided by the human utilisation of water resources.

The Djerid region is formed by about 30 oases, of which the most important are Tozeur, Nefta, Degache and Hazoua on the south flank of the Tozeur uplift, and Ibn Chabbat and El Hamma on the north flank.

The study area encloses Chott El Gharsa, Chott Djerid and the Tozeur uplift, which located between the two depressions. "Chott" is a North African term for a salt flat within a hydrologically closed basin (Gautier 1953; Shaw and Thomas 1997), and the elevation of a chott surface is controlled by the position of the water table and associated capillary fringe. The Chott El Gharsa (620 km^2) and Chott Djerid (5,360 km^2) are formed during Late Miocene–Early Pleistocene time as a result of compression between the African and European lithospheric plates (Swzey 2003).

Published online: 13 December 2011

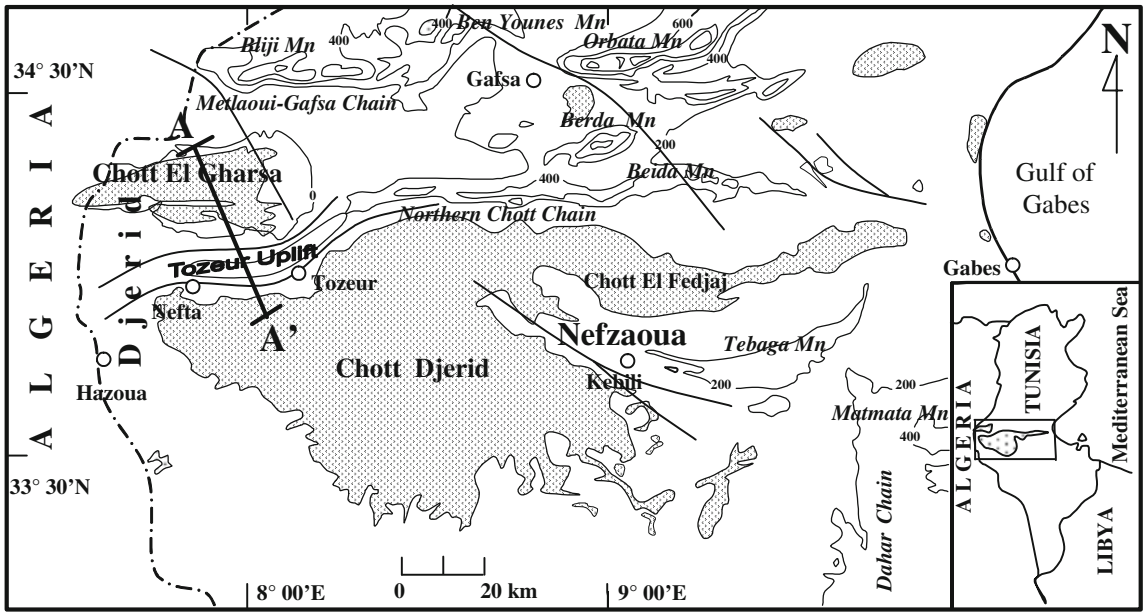

Fig. 1 Study area in southeastern Tunisia with geographic features with cross-section AA′ location

The centre of the Chott El Gharsa lies at −20 to −30 m below sea level, whereas altitude of Chott Djerid is 10–20 m above sea level (Swzey 2003) (Fig. 1).

Chotts are considered to function as evaporation pumps. The surface distribution of evaporites and the distribution of subsurface sediments are often related to artesian sources at the centres or at the edges of the basins (Schulz et al. 2002).

The drainage network in the region consists of El Khanga wadi (about 50 l/s). Melah and Tseldja are non-perennial rivers. El Khanga River is derived from the springs of the Upper Cretaceous and Miocene Groundwater. Melah and Tseldja wadi collect the surface runoff from surrounding hills. Chott El Gharsa constitutes the discharge area of these wadis (Fig. 2) (Coque 1962).

In the Djerid region, oases area increased from single to double in 30 years (1972–2004) by the extension of the old one and the creation of new oases to reduce increasing unemployment, affecting the extreme water and soil resources in the region (Kamel 2007).

The study area is characterised by an arid climate and by variable weak and irregular precipitation. Hydroclimatic data (precipitation, evapotranspiration and temperature), recorded at the Nefta and Tozeur meteorological stations, were acquired since 1897 with many gaps. The statistical analysis of the 1950–2004 mean inter-annual precipitation series revealed a good adjustment with the Gaussian-logarithmic probability law, with an average value of 91 mm at Nefta city and 101 mm at Tozeur city (Kamel 2007). The mean annual temperature prevailing in the area is about 21°C, but the difference between the highest and the lowest daily temperature may reach 15°C between January and July. Data on evaporation and evapotranspiration are very scarce. Few measurements were recorded by the National Office for Meteorology (ONM 2010) and Bryant (1999). Figures recorded at Tozeur station between, 1969 and 1972, revealed a mean inter-annual rate of 2,101 mm/year for evaporation (UNESCO 1972). On the other hand, mean annual evapotranspiration, as estimated by means of empirical formula such as those of Thornthwaite, Turc and Penman, gave results ranging from 1,275 (year 1991) to 1,806 mm (year 1989) per year between 1984 and 1991 (ONM 2010). In southern Algeria, at about 100 km western study area, the evaporative losses from the phreatic aquifer through a 6-m thick unsaturated zone were estimated to be 2 mm/year (Guendouz et al. 2006).

The main objectives of this paper is to provide a better understanding of mechanisms that contribute to water table Plio-Quaternary hydrodynamism and its mineralisation in the Djerid region using a large amount of data to verify assumptions regarding these mechanisms. Overexploitation 6 months/year (from April to September) and the vicinity of the brine Chotts aquifer are taken into account.

The new isotopic signal of precipitation in the Nefta oasis (Kamel 2011) helps to provide more information about PQ water table origin in the study area.

Hydrogeology

Regional aquifer system characteristics

In southern Tunisia, the aquifer system is composed of two trans-border major large Saharan and local limited shallow aquifers: the Continental Intercalaire (CI) overlain by the

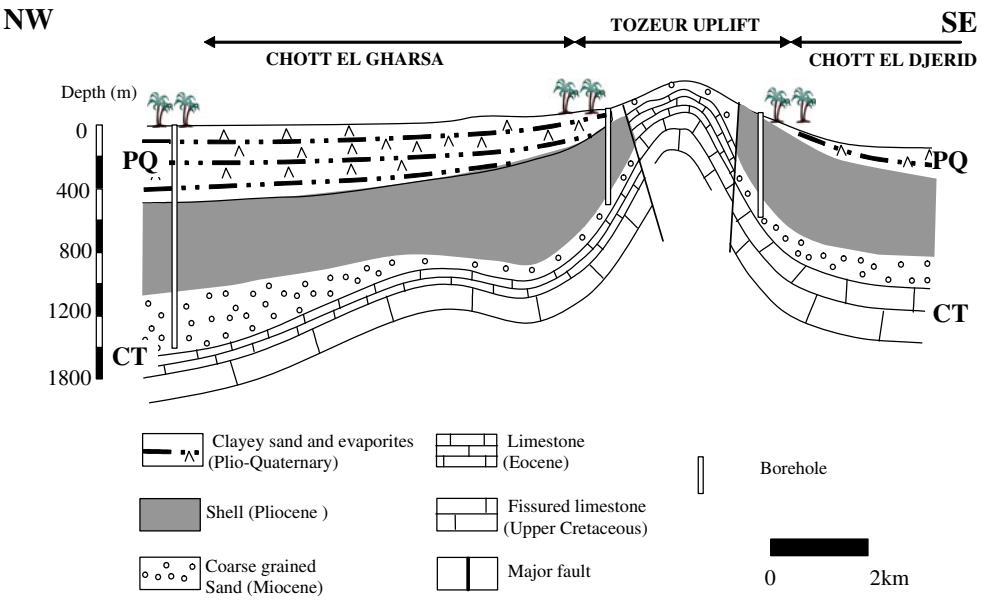

Fig. 2 Hydrogeological cross-section AA′, as indicated in Fig. 1

Complexe Terminal (CT) (UNESCO 1972). Both are shared between Algeria, Tunisia and Libya covering a surface of about 1 million km^2 (OSS 2003). The existence of the shallow Plio Quaternaire water table (PQ) is quasi limited to the oases area. The CI aquifer is one of the largest confined aquifers in the world. This immense multilayered aquifer is hosted in the continental formations of the Lower Cretaceous (Castany 1982). Its depth reaches locally 2,600 m, while its thickness ranges between 150 and 200 m in the study area. Twenty deep boreholes exploited the deep geothermal (water temperature ranges between 38°C and 75°C) CI aquifer between Chott Djerid and Chott El Gharsa. Their flow rates vary from 20 to 150 l/s, and they are mainly used for geothermal purposes and oases irrigation (Kamel et al. 2005).

The CT aquifer is hosted in the Upper Cretaceous carbonates and the sandy Miocene formation. The two aquifer horizons are separated by semi-permeable strata (OSS 2003). In the Djerid region, about 80% of agricultural and domestic water supply is provided by the sandy Miocene formation between 100 and 700 m depth drying up.

Transmissivity of the CT aquifer, obtained from pumping tests, ranges from 0.1×10^{-2} to 4.5×10^{-2} m^2/s in the sandy Miocene formation (Kamel et al. 2005). Overexploitation of the CI and CT aquifers for agricultural practices has contributed to loss of the artesian condition and springs; however, upward leakage to the phreatic aquifer can still occur due to head difference between large CI and CT Saharan and the locally shallow Plio-Quaternary aquifer.

Plio-Quaternary aquifer

At the surface, the Plio-Quaternary formations contain the phreatic waters. It is mainly composed of fine grain size aeolian sand and sandy clay with gypsum in the subsurface.

These sands generally are homogeneous of fine to medium granulometry and are poorly cemented. This is at the origin of disintegration and the collapse observed in many shallow dugs (Kamel 2007).

It may also contain locally at the top 0.5–1.5-m thick layers of saline gypsum crust.

The crust and bedded gypsum deposits at water table level cover a relatively large surface of south Tunisia and in particular the oases (Bureau et Roederer 1960; Pouget 1968) (Fig. 2). At the base, the PQ formed by compact clay 300-m thick corresponding to the top of the confined CT aquifer, in the Hazoua region, near the Algerian frontier. From east to west, clay becomes increasingly compact and thick (Kamel 2011).

The PQ aquifer depth varies from 10 to 40 m in oases area to reach locally 400 m at the northern margin of Chott El Gharsa (Fig. 3). It is exploited at about 4 millions m^3/year through more than 2,000 dug wells, not exceeding 50 m depth. Transmissivity of the PQ aquifer, obtained from Porcher short pumping tests, ranges from 3×10^{-3} to 5.5×10^{-4} m^2/s in the clayey sand formation (Kamel 2007).

In the PQ aquifer, the groundwater flow converges from Tozeur uplift to the Chott El Gharsa, at north and toward chott Djerid at south, which constitute the natural discharge areas of the PQ aquifer (Fig. 4). In the CT aquifer, the main flow directions are observed from the southern Atlas Mountains of Algeria (toward Nefta and Tozeur oases) and from the Dahar uplands (Tunisia) to the eastern part of the study area (Fig. 4) (Kamel 2007). The discharge area is Chott Djerid where numerous springs (aiouns) are to be found supplied by water rising through the Mio-Plio-Quaternary sequence (Castany 1982).

In the Djerid oases, potentiometric CT surface and water table PQ contour are almost at the same pressure (Fig. 4),

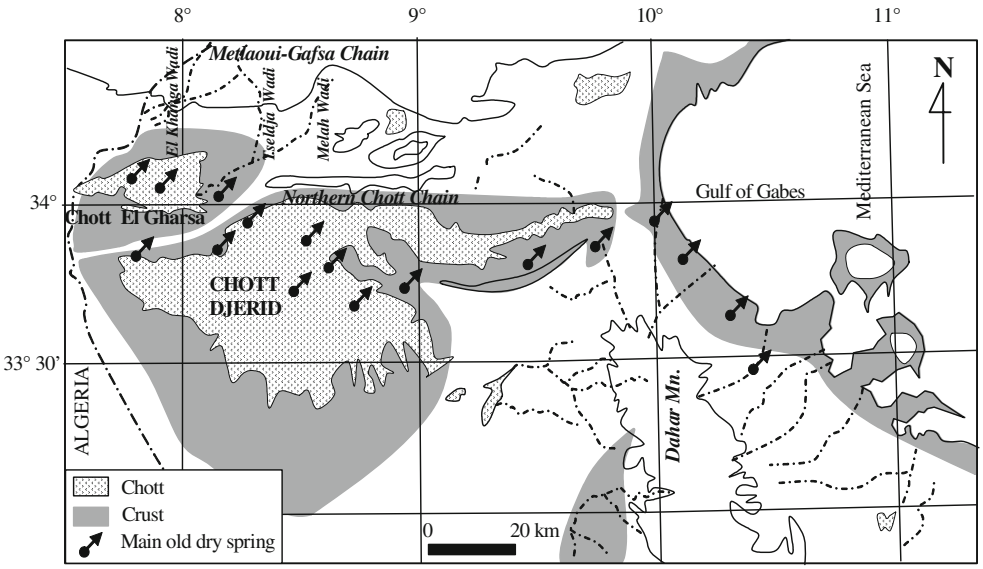

Fig. 3 Distribution of gypsum crust with the main old dry springs and the drainage network (after Pouget 1968 modified)

and the balance governed by the exploitation status of these aquifers remains very fragile.

Chotts hydrological system

The Chott Djerid and Chott El Gharsa, in southern Tunisia, are contemporaneous terrestrial, evaporitic environment that have been the subject of intense sedimentological and hydrochemical studies (Coque 1962; Gueddari et al. 1983; Millington et al. 1989; Drake et al. 1994; Swzey 2003; Hammi et al. 2003). The Chott Djerid has a surface area of approximately 5,360 km^2 (Millington et al. 1989) and Chott El Gharsa of about 620 km^2.

The centre of Chott El Gharsa lies at −20 to −30 m below sea level, whereas altitude of Chott Djerid is 10–20 m above sea level (Swzey 2003).

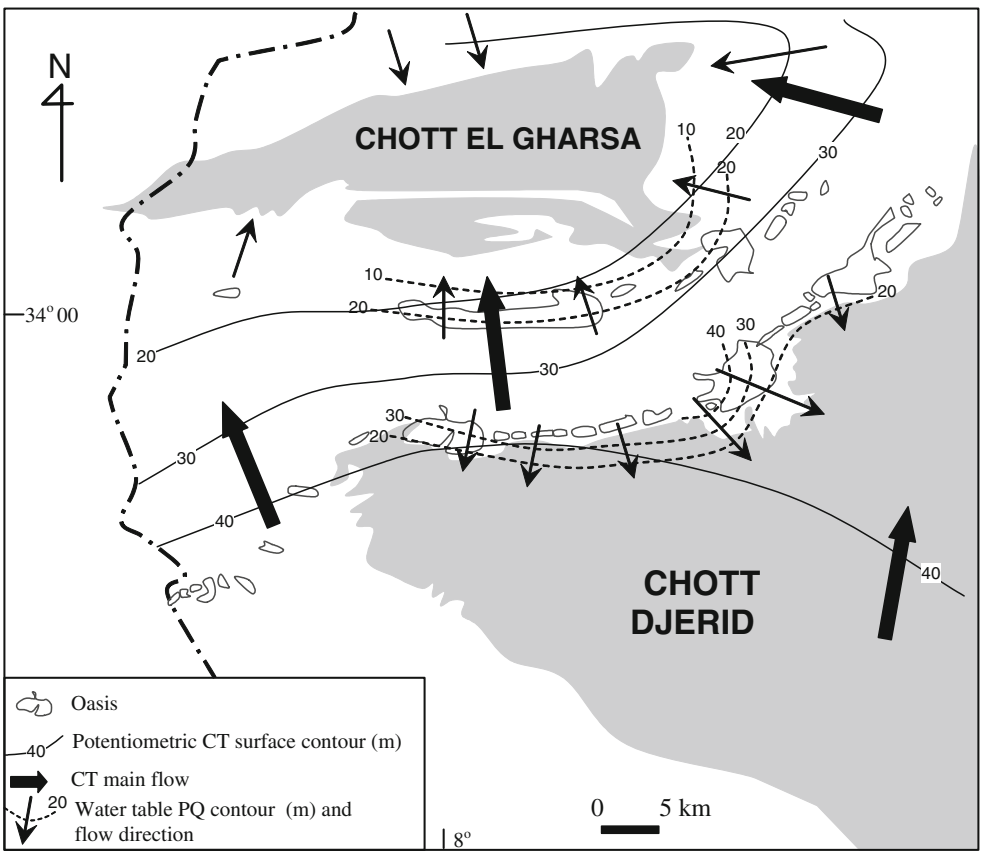

Fig. 4 Comparative maps of potentiometric CT and water table PQ contour in the Djerid region (2007)

The Chott Djerid is a playa with a groundwater province considerably larger than its topographic basin; fluctuations in groundwater level should be largely controlled by the balance between artesian recharge and evaporation (Drake and Bryant 1994). This is supported by observations of surface water on the Chott between 1947 and 1958 (Coque 1962; Drake and Bryant 1994). Some contemporary observations show that, during most years, at least part of basin is covered between the months of November and February, a period in which aquifer resurgence within the basin is most likely to be greater than evaporation. However, although probably constant until the last century, the flow from the Continental Intercalaire and the Complexe Terminal aquifers has been observed to have reduced significantly as a result of systematic abstraction over the 100 years (Mamou 1989). Such a reduction in groundwater inflow suggests that seasonal lake formation resulting from effective precipitation may be less common at present than in the period prior to extensive Saharan aquifers abstraction.

Consequently, in southern part of the Djerid oases, in the vicinity of the Chott margin, there is deterioration in water quality in the Plio-Quaternary aquifer. This is caused mainly by evapotranspiration and the subsequent down-gradient migration of the saline Chott brine. There is indication from some wells that this may be only a superficial feature and that an improvement in water quality with depth beneath the oases may occur.

Retention of water within the playa is generally a function of evaporation rates, subsequent precipitation events and groundwater outflow/seepage (Bryant 1999)

The inundation process within a saline pan has been observed to take place in four successive stages: inundation, evaporative concentration of the water body, the formation of shallow brine pools and final dessication of surface water to the precipitation of a salt crust (Bryant et al. 1994).

Analytical methods

A representative set of samples was collected from 169 active agricultural water supply dugwells penetrating the Plio-Quaternary aquifer, from 4 to 50 m depth between 2007 and 2011 (Table 1 and Fig. 5) in 13 oases (Fig 5). Temperature, electrical conductivity and pH were measured in the field (Table 1). Major element determination was carried out on samples filtered through 0.45 μm. The geochemical analysis were carried out in the 'laboratoire du CRDA de Gabes and Laboratoire du groupe Chimique Tunisien' included flame atomic absorption analysis for all cations, ion selective electrode determination and colorimetric analysis using Standard methods. The saturation with respect to involved mineral in mineralisation mechanisms of all sampled water were determined using the WateqF subroutine program (Plummer et al. 1979).

Stable isotopes of oxygen and hydrogen were determined using isotope ratio mass spectrometry for 36 samples. Hydrogen and oxygen isotope analyses were made by respectively employing the standard CO_2 equilibration and the zinc reduction technique (Epstein and Mayeda 1953), followed by analysis on a mass spectrometer. All oxygen and hydrogen isotope analyses are reported in the usual d notation relative to Vienna standard mean oceanic water (SMOW) standard. Typical precisions are±0.2‰ and±2‰ for the oxygen and deuterium, respectively.

Results and discussion

Physico-chemical data

The conductivity of PQ groundwater samples range from 2,320 to 32,600 μS/cm. The highest values are measured in samples from the northern side of Chott El Gharsa, where some dug wells are abandoned (Table 1). The salinity of PQ aquifer in the Djerid and Nefzaoua regions increases in time (Zamouri et al. 2007). High groundwater CT abstraction in this region to ensure agricultural purposes including water for increasing tourism needs (swimming pools) leads to formation of depression cone, which facilitates leakage of brine from the local shallow Chott groundwater saline. In the Dhafria region, the salinity of groundwater is abnormally high, suggesting saline water originating from Chott El Gharsa. The total dissolved solids (TDS) varies between 2.05 and 26.740 g/l with mean value of 13.200 g/l. The electrical conductivity and TDS were not homogeneous (Table 1), indicating that the PQ waters differed considerably probably due to recharge in local perched aquifer for low salinity and the mixing by brine of the Chotts or leakage with underlying aquifer with evaporite dissolution during fluxes ascent for high salinity.

PQ samples were collected from dug wells not exceeding 50-m depth, and water temperature was in the same range of ambient temperature, between 21°C and 30°C. The pH of PQ groundwater ranged between 6 and 8 (Table 1), an indication that the dissolved carbonates were predominantly in the HCO_3 form (Adams et al. 2001).

Water types

Chemical composition of the analysed groundwater samples is plotted on the Chadha diagram (Chadha 1999), which is a somewhat modified version of the Piper diagram and the expanded Durov diagram (Chadha 1999). The plot of the PQ groundwater samples in the Chadha diagram (Fig. 6) present two groups. The first group (A), which comprised the majority of the analysed samples, showed that the

Table 1 Physico-chemical and isotopic data of groundwater

Number of oasis	Number of samples	Statistics	pH	C (mS/cm)	TDS (g/l)	Ca (mg/l)	Mg (mg/l)	Na (mg/l)	K (mg/l)	SO_4 (mg/l)	Cl (mg/l)	HCO_3 (mg/l)	^{18}O (‰ vs SMOW)	^{2}H (‰ vs SMOW)
1	5	Minimum	6.5	5.82	4.93	619	205	482	14	2111	532	103	−5.13	−49.2
		Maximum	7.4	10.80	8.65	879	311	1195	31	3071	2129	426	−4.24	−45.7
		Average	6.9	8.19	6.77	734	287	836	21	2629	1309	215	−4.60	−47.03
		SD	0.4	2.43	1.76	133	46	336	7	438	765	123	0.38	1.52
2	11	Minimum	6.7	6.53	5.27	535	105	316	25	1823	669	97	−5.33	−49.5
		Maximum	7.9	10.61	7.63	839	383	1689	78	2879	2484	749	−3.88	−39.5
		Average	7.3	8.02	6.30	724	278	695	38	2405	1197	292	−4.73	−46.91
		SD	0.3	1.34	0.84	83	89	443	16	312	635	173	0.42	3.08
3	1		7.4	8.84	6.87	639	239	1057	51	2111	1703	213	−3.81	−43.7
4	22	Minimum	7.0	3.54	2.86	260	120	324	15	998	572	185	−3.49	−42.4
		Maximum	7.9	21.06	18.84	871	886	4140	183	4800	7043	495	−3.2	−41,00
		Average	7.4	8.17	7.29	555	358	1112	58	2735	1687	317	−3.35	−41.7
		SD	0.4	3.75	3.40	134	181	826	43	947	1342	93	0.14	0.70
5	10	Minimum	7.0	6.58	4.74	380	225	589	17	1679	923	83	−5.05	−43.1
		Maximum	8.1	21.80	19.42	779	791	4531	187	7056	5943	365	−3.54	−42.6
		Average	7.3	10.87	8.99	563	380	1818	62	3606	2326	230	−4.1	−42.85
		SD	0.3	4.58	4.56	132	178	1226	47	1835	1451	78	0.83	0.35
6	11	Minimum	7.0	5.63	5.18	506	238	658	33	1704	1056	155		
		Maximum	7.3	9.90	7.69	650	358	1103	96	3144	1952	356		
		Average	7.1	7.09	6.38	545	292	875	53	2561	1370	255	−4.24	−44.8
		SD	0.1	1.14	0.73	50	48	155	19	384	255	54		
7	1		7.4	9.75	7.67	551	298	1011	16	2879	1596	139	−5.24	−37.6
8	1		7.7	6.22	5.19	679	287	298	31	2303	638	152	−4.59	−46.1
9	11	Minimum	7.0	6.40	5.88	444	254	367	33	2328	1064	196	−4.62	−47.4
		Maximum	8.0	13.00	12.28	919	618	2070	71	4656	3037	409	−3.69	−43.6
		Average	7.5	9.18	7.87	680	390	958	49	2971	1675	285	−4.28	−45.42
		SD	0.4	1.79	1.80	171	115	543	12	688	589	63	0.43	1.83
10	16	Minimum	7.1	2.90	2.42	304	115	276	8	1180	355	11		
		Maximum	8.3	26.40	22.89	751	709	5749	54	9263	5608	590		
		Average	7.7	7.92	7.04	522	259	1268	18	3190	1280	151	−6.81	−47.1
		SD	0.2	6.10	5.32	125	170	1430	14	1996	1507	126		
11	5	Minimum	7.4	3.30	2.99	359	119	187	10	1458	283	157	−6.61	−47.1
		Maximum	8.0	5.76	4.25	543	215	530	18	2087	674	261	−4.51	−30.1
		Average	7.7	4.17	3.59	485	174	373	13	1846	461	212	−5.56	−38.6
		SD	0.2	1.06	0.49	84	41	152	3	251	174	42	1.48	12.02
12	41	Minimum	7.2	0.94	2.04	255	95	263	3	1016	212	51	−6.66	−48.7
		Maximum	8.6	32.50	26.73	767	1133	5749	150	6335	9051	408	−5.82	−36.7
		Average	7.8	11.06	9.58	572	456	1700	27	3845	2104	169	−6.15	−44.26
		SD	0.2	5.29	4.07	87	196 945	25	1159	1444	79 0.44	4.59		
13	34	Minimum	7.4	3.51	3.20	320	57	248	12	1344	284	34		
		Maximum	7.9	10.43	7.72	768	451	1575	47	3936	627	292		
		Average	7.6	6.23	4.91	509	204	828	27	2128	1149	164	–	–
		SD	0.1	1.85	1.28	97	93	387	10	511	588	42		

alkaline earth (Ca+Mg) exceeded the alkali metals (Na+K) and that the strong acids (Cl+SO_4) exceeded the weak acid (HCO_3). The second group (B) revealed that (Na+K) was superior to (Ca+Mg) and the strong acids (Cl+SO4) exceeded the weak acid (HCO_3). Group A is Ca–Mg–SO_4/Cl water type and group B is Na–Cl water type. The evolution of water facies from sulphated group A in the oases to chloride group B in the vicinity of Chotts is evidenced in the Chadha diagram (Fig. 6)

Major ions geochemistry and saturation states

Decline of CT Saharan piezometric head due to influence of long-term over-pumping, in the Djerid region, in response to

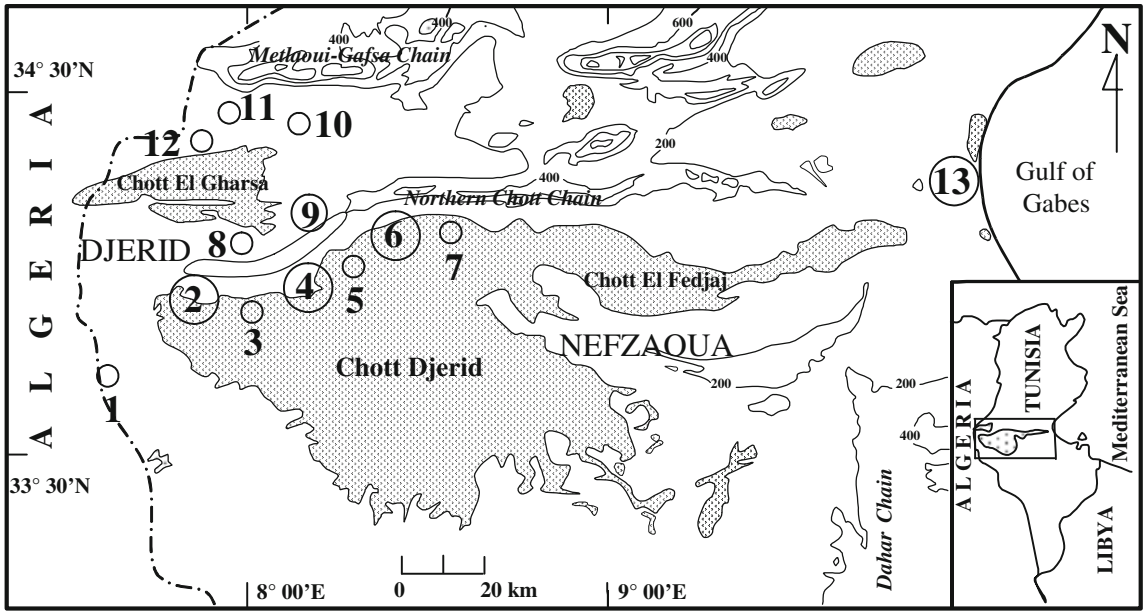

Fig. 5 Location of sampled dugwells in 13 oases in Southern Tunisia. *1* Hazoua, *2* Nefta, *3* Mrah Lahouara, *4* Tozeur, *5* Castilia/Manachi, *6* Degache, *7* Ceddada, *8* Ibn Chabbat, *9* Chemsa/El Hamma, *10* Segdoud, *11* El Oudia, *12* Dhafria and *13* Gabes

the large extension of the agricultural areas, has contributed to deleterious and irreversible consequences including the drying of all springs and the PQ water quality degradation due to the crust formation. Dissolution of crust by return flow irrigation and sporadic precipitation largely define the chemical composition of the PQ groundwater.

Major reactive sulphate salts associate to the crust are mainly gypsum ($CaSO_4.2H_2O$), anhydrite ($CaSO_4$), epsomite ($MgSO_4{\cdot}7H_2O$), burkeite ($Na_2CO_3{\cdot}2Na_2SO_4$), thenardite (Na_2SO_4), mirabilite [$Na_2SO_4{\cdot}10(H_2O)$]. Halite (NaCl) and magnesium chloride ($MgCl_2$) constitute the main chloride salt of the surface and subsurface crust.

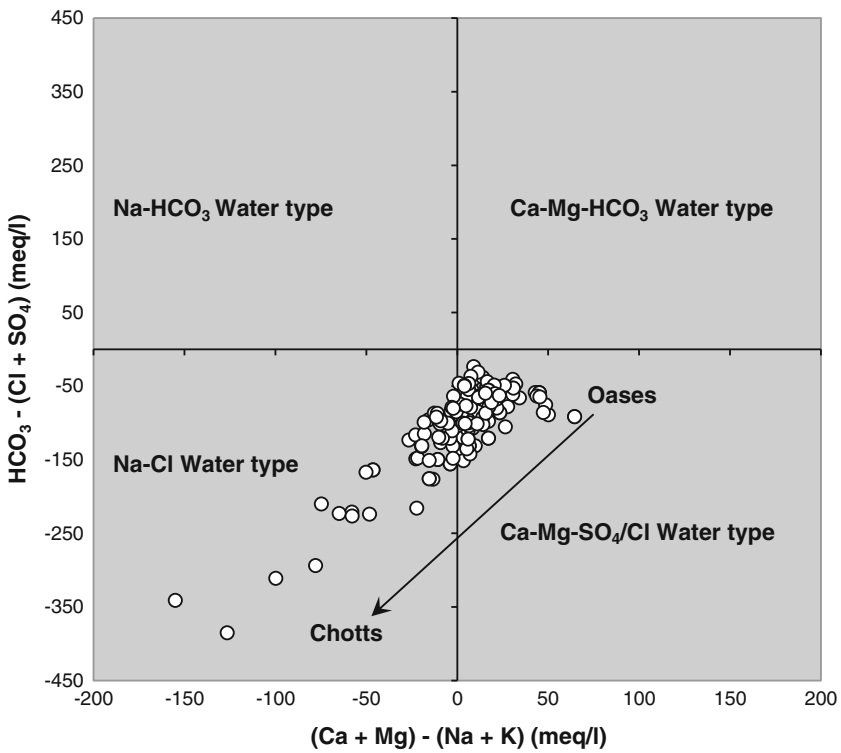

Fig. 6 Chadha diagram showing the water type of the groundwater samples

The computed SI values showed that groundwater in the PQ aquifer was largely undersaturated with respect to halite, thenardite, mirabilite and, to a lesser extent, with respect to anhydrite and gypsum, indicating possible dissolution of these minerals (Table 2).

These eventual dissolutions were confirmed by strong positive relationships of Na versus Cl, Na_2 versus SO_4, Mg versus Cl_2 and Mg versus SO_4 (Fig. 7). Positive correlations between the SI of referred dissolved minerals and some ions resulting from each dissolution are shown in Fig. 8.

Table 2 Saturation indexes of main minerals

Number of oasis	Number of samples	Statistics	$SI_{Anhydrite}$	$SI_{Aragonite}$	$SI_{Calcite}$	$SI_{Dolomie}$	SI_{Gypsum}	SI_{Halite}	$SI_{Mirabilite}$	$SI_{Thenardite}$
1	5	Minimum	−0.236	−0.387	−0.243	−0.552	−0.011	−5.039	−4.662	−5.443
		Maximum	−0.077	0.795	0.939	1.947	0.138	−4.348	−3.914	−4.835
		Average	−0.162	0.098	0.234	0.444	0.073	−4.656	−4.252	−5.124
		SD	0.079	0.573	0.497	1.061	0.077	0.361	0.394	0.325
2	11	Minimum	−0.322	−0.418	−0.275	−1.034	−0.106	−4.561	−4.837	−5.763
		Maximum	−0.117	0.948	1.092	2.152	0.067	−4.128	−3.643	−4.563
		Average	−0.223	0.321	0.465	0.748	−0.044	−4.394	−4.1794	−5.103
		SD	0.092	0.522	0.522	1.349	0.096	0.186	0.429	0.432
3	1		−0.280	0.506	0.650	1.255	−0.063	−4.477	−4.110	−5.034
4	22	Minimum	−0.730	−0.169	−0.025	−0.035	−0.522	−5.431	−5.117	−6.047
		Maximum	−0.213	1.013	1.157	2.492	−0.004	−3.344	−2.859	−3.758
		Average	−0.348	0.352	0.453	0.969	−0.195	−4.805	−4.377	−5.301
		SD	0.152	0.422	0.415	0.877	0.216	0.597	0.659	0.666
5	10	Minimum	−0.442	−0.389	−0.245	0.039	−0.232	−4.984	−4.179	−5.517
		Maximum	−0.057	1.373	1.517	3.025	0.152	−3.388	−2.616	−3.515
		Average	−0.260	0.302	0.435	1.178	−0.049	−4.268	−3.572	−4.593
		SD	0.114	0.640	0.539	0.994	0.121	0.453	0.563	0.629
6	11	Minimum	−0.382	−0.179	−0.035	0.006	−0.173	−4.839	−4.563	−5.486
		Maximum	−0.214	0.334	0.477	0.912	−0.005	−4.162	−3.951	−4.875
		Average	−0.274	0.062	0.227	0.586	−0.065	−4.628	−4.193	−5.112
		SD	0.045	0.151	0.152	0.259	0.048	0.204	0.207	0.196
7	1		−0.245	0.265	0.409	0.935	−0.028	−4.533	−4.017	−4.941
8	1		−0.188	0.737	0.880	1.769	0.033	−5.434	−5.128	−6.057
9	11	Minimum	−0.379	−0.070	0.074	0.313	−0.162	−5.133	−4.983	−5.909
		Maximum	−0.072	0.987	1.131	2.638	0.144	−3.985	−3.328	−4.243
		Average	−0.215	0.694	0.802	1.877	0.001	−4.601	−4.194	−5.141
		SD	0.097	0.383	0.394	0.899	0.097	0.389	0.588	0.558
10	16	Minimum	−0.567	0.342	0.486	0.883	−0.349	−5.669	−5.169	−6.098
		Maximum	−0.183	0.429	0.903	1.716	0.033	−4.325	−3.478	−5.243
		Average	−0.283	0.379	0.619	1.223	−0.075	−5.171	−4.374	−5.690
		SD	0.143	0.037	0.163	0.316	0.157	0.538	0.705	0.468
11	5	Mininmum	−0.495	0.461	0.604	1.103	−0.272	−5.963	−5.548	−6.478
		Maximum	−0.254	0.875	1.019	2.109	−0.036	−5.192	−4.642	−5.653
		Average	−0.340	0.737	0.881	1.690	−0.122	−5.523	−4.948	−6.039
		SD	0.099	0.161	0.162	0.364	0.096	0.366	0.412	0.378
12	41	Mininum	−0.688	0.073	0.045	0.271	−0.18	−5.913	−5.369	−5.517
		Maximum	−0.017	1.214	1.357	2.913	0.199	−3.107	−2.522	−3.834
		Average	−0.217	0.639	0.755	1.783	0.010	−4.333	−3.645	−4.564
		SD	0.112	0.285	0.300	0.612	0.085	0.475	0.543	0.388
13	34	Minimum	−0.534	−0.518	−0.375	−0.259	−0.317	−5.812	−5.308	−6.237
		Maximum	−0.173	0.855	0.999	1.795	0.044	−4.159	−3.557	−4.478
		Average	−0.349	0.365	0.521	1.008	−0.129	−4.836	−4.393	−5.313
		SD	0.105	0.265	0.245	0.437	0.109	0.429	0.426	0.426

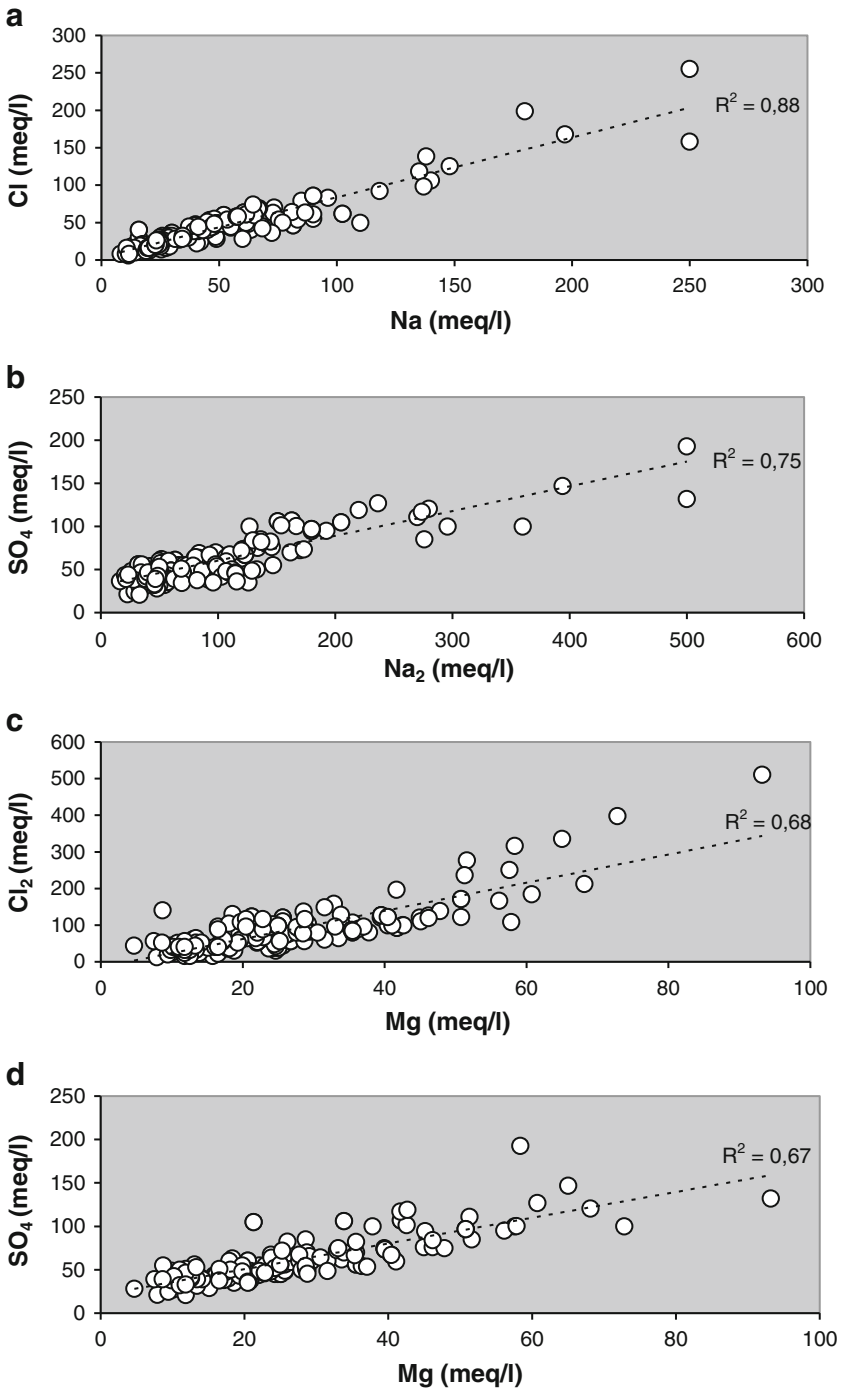

Fig. 7 Bivariate diagrams between major elements: Na/Cl (**a**), Na_2/SO_4 (**b**), Mg/Cl_2 (**c**) and Mg/SO_4 (**d**)

Normally, gypsum dissolution produces Ca and SO_4 in 1:1 equivalent ratio. However, for the PQ groundwater samples, the plot of SO_4 versus Ca (Fig. 9a) shows a relative Ca depletion. Thus, the deficiency of calcium is probably related to carbonate precipitation through two possible mechanisms. (1) carbonates replacing evaporites (anhydrite/gypsum) are microbially generated by bacterial sulphate reduction, based on 13^C values that support an organic origin of the carbon (Henchiri and Slim-S'Himi 2006). (2) Since all groundwater samples are saturated with respect to calcite (Fig. 8d) and dolomite (Table 2) and undersaturated with respect to gypsum and anhydrite (Fig. 8b), the dissolution of anhydrite continues and the concentration of Ca^{2+} and SO_4^{2-} increase to reach supersaturation and precipitation, which may decrease Ca^{2+} concentrations (Fig. 9a). The decrease in HCO_3^- concentrations, resulting also from calcite precipitation, may then cause de-dolomitisation process, adding Mg^{2+} to the waters and decreasing the Ca/Mg molar ratios (Marfiaa et al. 2004). This process, which is evidenced by the 1:1 relationship in the plot of $(Ca^{2+}+Mg^{2+})$ versus $(SO_4^{2-}+0.5HCO_3^-)$ (Fig. 9b) (Mc

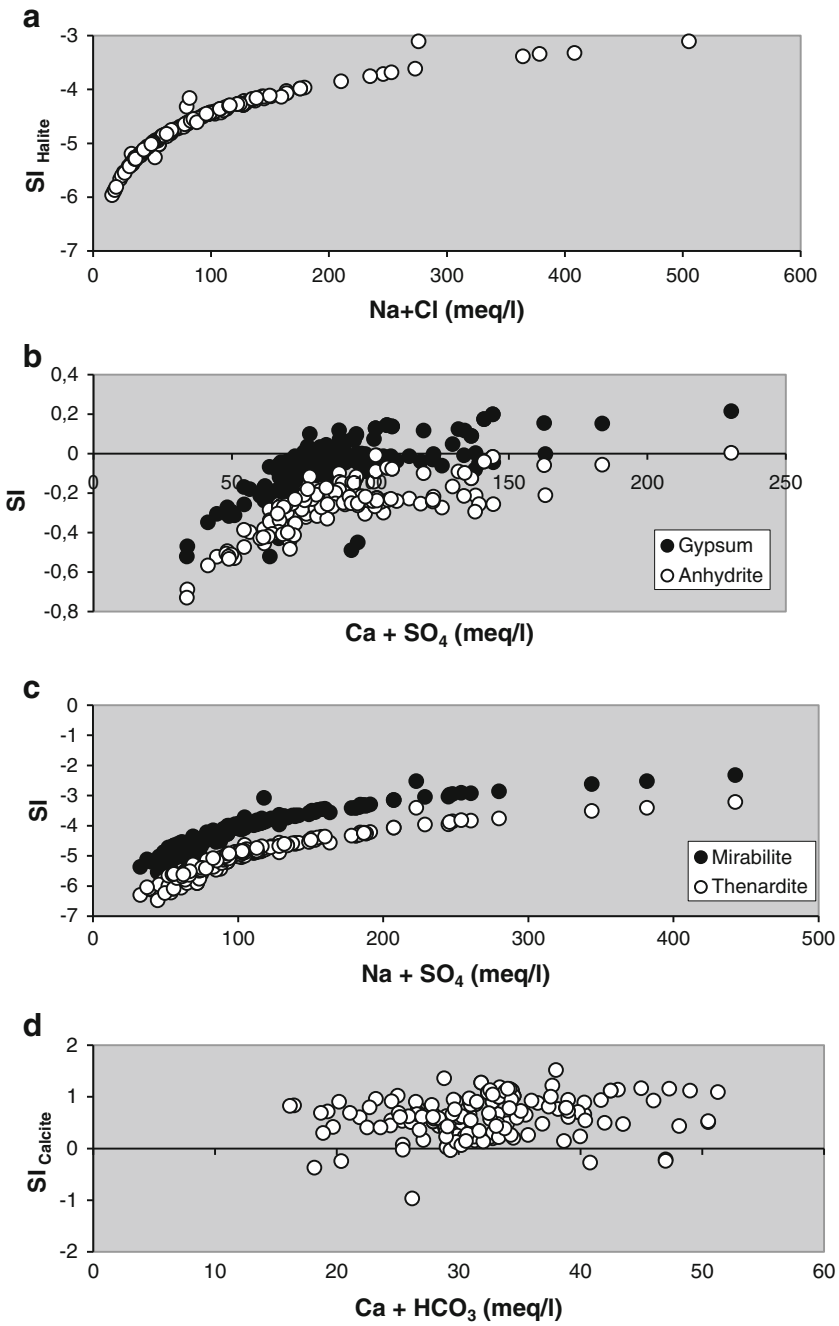

Fig. 8 Mineral saturation indexes versus representative species relationship; SI_{Halite}/(Na+Cl) (**a**), SI/(Ca+SO_4) (**b**), SI/(Na+SO_4) (**c**) and $SI_{Calcite}$/(Ca+HCO_3) (**d**)

Intosh and Walter 2006), corresponds to the incongruent dissolution of dolomite to form calcite with a crystalline structure similar to dolomite. Calcite formed in this way is called 'dedolomite' (Hanshaw and Back 1979). The net reaction for the de-dolomitisation process is (Mc Intosh and Walter 2006):

$$CaMg(CO_3)_2(s) + CaSO_4 \cdot 2H_2O(s) + H^+ = CaCO_3(s) + Ca^{2+} + Mg^{2+} + SO_4{}^{2-} + HCO_3{}^- + 2H_2O$$

On the other hand, cation exchange probably generates a Ca deficiency with respect to SO_4 concentration. The phenomenological evidence for this exchange is given by the bivariate plot of (Ca+Mg)−(HCO_3+SO_4) in function of (Na+K−Cl) (Garcia et al. 2001) as shown in Fig. 10. In the absence of these reactions, all data should plot close to the origin (Mc Lean et al. 2000). However, Fig. 10 indicates an increase in (Na+K) related to decrease in (Ca+Mg).

Isotopic study

Assuming no meaningful variation of stable isotope content in CT groundwater in the Djerid region since 1982 (Zouari et al. 2006), data of all groundwater samples were plotted

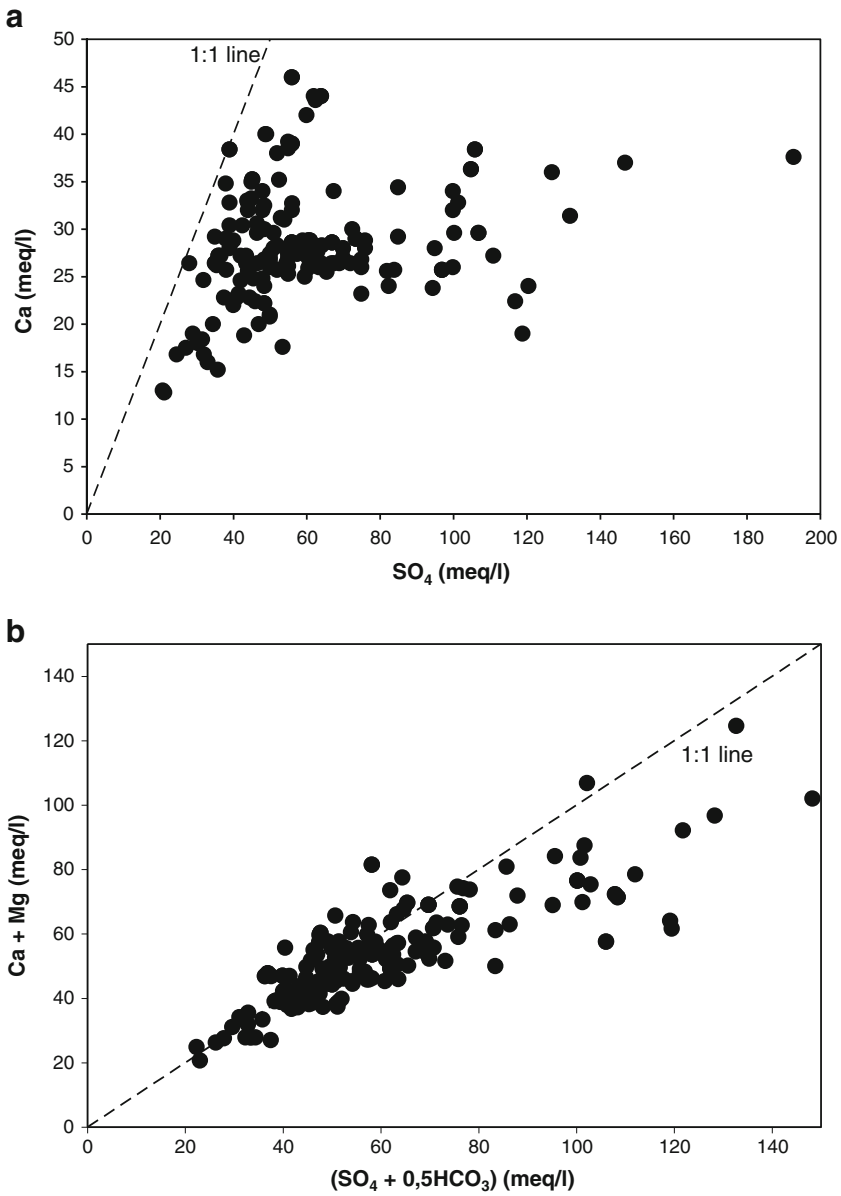

Fig. 9 Bivariate diagrams between SO_4/Ca (**a**) and (Ca+Mg)/(SO_4+0.5 HCO_3) (**b**)

together with the Global Meteoric water Line, Nefta local meteoric Water Line and weighted mean precipitation for Nefta obtained from 2000 to 2003. Additional data concerning the underlying deep confined CI and confined/unconfined CT aquifers were used, including their respective weighted mean values of stables isotope contents (Edmunds et al. 2003; Kamel et al. 2005).

Data from the PQ varied in relatively wide range from −6.8‰ to −3.19‰ for $\delta^{18}O$ and from −49.4‰ to −30.0‰ for $\delta^{2}H$. The weighted means values of $\delta^{18}O$ were −3.17 for the precipitations, and −7.5 for the CI and −5.44 for the CT. Those of the $\delta^{2}H$ are −22.26 for the precipitation, −59.6 for the CI and −49.5 for the CT (Fig. 11).

Figure 11 shows a depleted pole enclosing mean CI and CT borehole wells and a group enclosing the PQ water samples (with two subgroups 3 and 4). Mean CT, CT and PQ isotopic data define a line with a slope of about 4, which can be interpreted as an evaporation line (Kamel et al. 2007). The intersection of this evaporation line with the local meteoric water line gives values of −9‰ and −67‰ for respective $\delta^{18}O$ and $\delta^{2}H$ contents of recharging precipitation before evaporation. The origin of these waters is presumably from recharge during a cool regime in the past. This observation agrees with the results of several authors obtained in southern Tunisia, which were interpreted as recharge occurring during the late Pleistocene and the early Holocene periods (Fontes and Edmunds 1989; Edmunds et al. 1997, 2003; Zouari et al. 2003, Kamel et al. 2007).

The referred evaporation line coincides practically with the mixing line of CI-CT and CT-PQ groundwaters. The

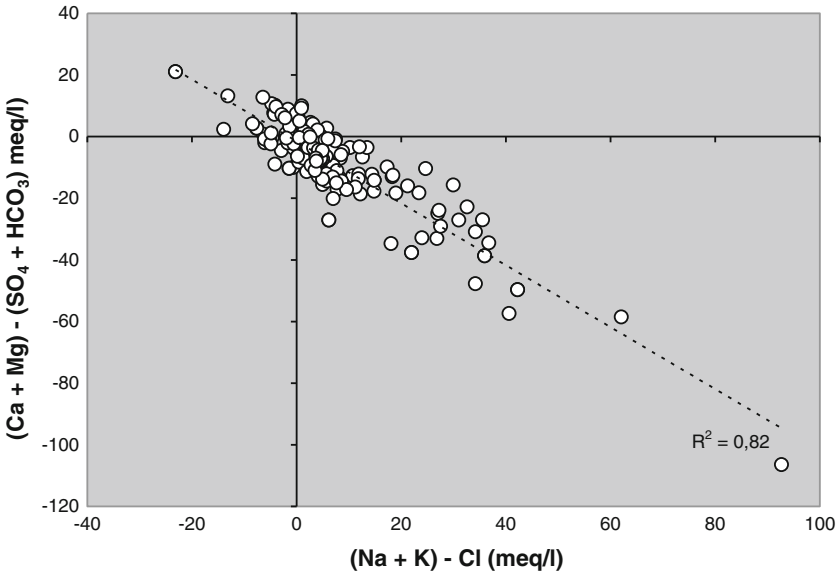

Fig. 10 (Na+K)−Cl/(Ca+Mg)−(SO_4+HCO_3) relationship

coincidence of the referred evaporation and mixing lines seems to be due to the common old origin of the CT and PQ groundwaters. In fact, the main source of recharge of the PQ aquifer is insured by the return flow of irrigation waters, which exploits about 150 Mm^3/year pumped from the CT reservoir. Thus, the excess irrigation water returns to PQ aquifer and mixes with water from the regional groundwater flow system.

In the detail, PQ groundwater samples form two subgroups, with $\delta^{18}O$ contents greater than −4‰ for the first more enriched one (group 4) and between −5.32‰ and −4.23‰ for the second (group 3).

The δ^2H and $\delta^{18}O$ of the return flow water fractionate and concentrate at different rates in the irrigation channels under two main irrigation conditions: (1) within the oases where there is a microclimate with low evaporation (group

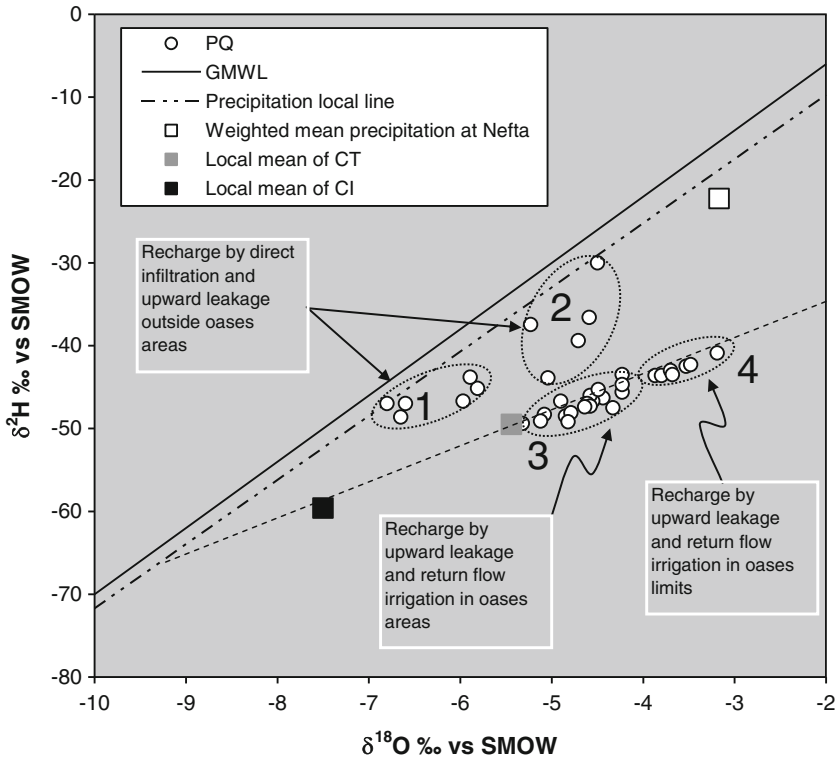

Fig. 11 $\delta^{18}O$ versus δ^2H diagram for sampled dugwells

3) and (2) in oases margin where the density of palm trees is low and the evaporation is the highest. This provides to the CT groundwater return flow an evaporated apparent character (group 4). The old origin of the PQ groundwater is also confirmed by the position of the representative points in the $\delta^2H/\delta^{18}O$ diagram, which fall largely below the global and the Nefta meteoric lines. However, some modern recharge of this shallow aquifer is indicated by the position of some samples closer to the GMWL and Nefta local Line (groups 1 and 2).

This subdivision into two subgroups is consistent with the subdivision made in the Oued Souf phreatic aquifer (Algeria) on the basis of tritium contents (Guendouz et al. 2006). The Djerid and Oued Souf regions are both of the Great Oriental Erg Basin. Oued Souf is only 80 km west of the study area.

Stable isotope/chloride relationship

The contribution from the CT aquifer recharging the PQ water table does not take place in a homogeneous manner throughout the Djerid region. It depends mainly on the irrigation rate inside or at the margin of oasis and the architecture of the reservoir, which control the upward leakage (Kamel 2011).

The distinguishing between the two mineralisation processes, dissolution and evaporation, can be assumed when plotting Cl concentrations against $\delta^{18}O$. Figure 12 shows the different trends displayed in the $\delta^2H/\delta^{18}O$ relationship. Figure 12 shows two poles where the mineralisation by dissolution dominates (group 1); the other pole is defined by samples collected at the oases margins where the PQ is recharged by CT evaporated return flow (group 4).

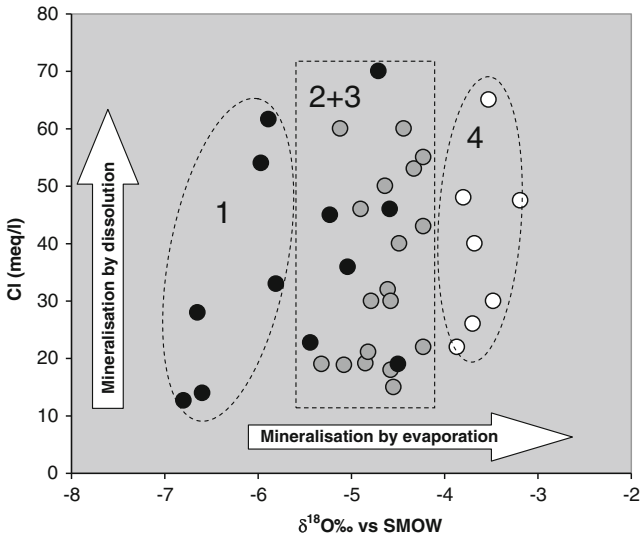

Fig. 12 $\delta^{18}O/Cl$ relationship

Groups 2 and 3, defined in Fig. 11, falls on the same isotopic content range reflecting the probable double origin of PQ water table inside oases, i.e. recharge by non-evaporated CT return flow irrigation and mixing by sporadic precipitation events.

Conclusions and recommendations

In the Tunisian Chotts region, which constitutes the discharge area of the two large CI and CT Saharan aquifers, the groundwater flow runs out toward closed basins. Groundwater flows occur by rising upward along the major faults as springs and by vertical upward leakage due to the difference in the potentiometric heads between the various aquifer levels through aquitards. In these large closed basins, evaporation creates large areas of salt crusts, called Chotts. On the edge of these Chotts, springs from the CT groundwater, give rise to oases.

Population growth, the extension of the old oases and the creation of new oases led to the drying up of springs and continuous lowering of groundwater level. The creation of boreholes more and deeper, tapping the Saharan aquifers to meet the growing need for irrigation has two consequences: (1) decompression of the Saharan groundwaters and decrease of its hydrological performances and (2) creation of perched water table, known as 'oasis type' mainly recharged by CT return flow irrigation and sporadic rare precipitation events. Oasis type water table was classified as secondary role and exploited mainly in summer period as supplementary irrigation, when evaporation becomes most significant of the year.

In the Djerid region, the exploitation of this water table reaches on average 4 billion m^3 per year and may cause a reverse flow of brines Chotts (that can fill up and become real salt take during rainy years) to the referred shallow aquifer, which is gradually becoming saline and unsustainable with consumption.

The conceptual model in Fig. 13 summarises very schematically (without regard to paleo crusts) the different stages of the hydrodynamic and geochemical evolution of PQ water table and its eventual contamination by the brines chotts.

Before the 1970s, the last century, springs and some boreholes tapping the CT aquifer provided water irrigation old oases needs.

At that time, potentiometric head CT reaches the top of Tozeur uplift and feed power springs with 800 l/s in the beginning of the last century (Mamou 1989) (stage1, Fig. 13).

Between 1970 and 2000, overexploitation of the CT aquifer has contributed to the loss of the artesian conditions and the decline of groundwater CT level. The return flow

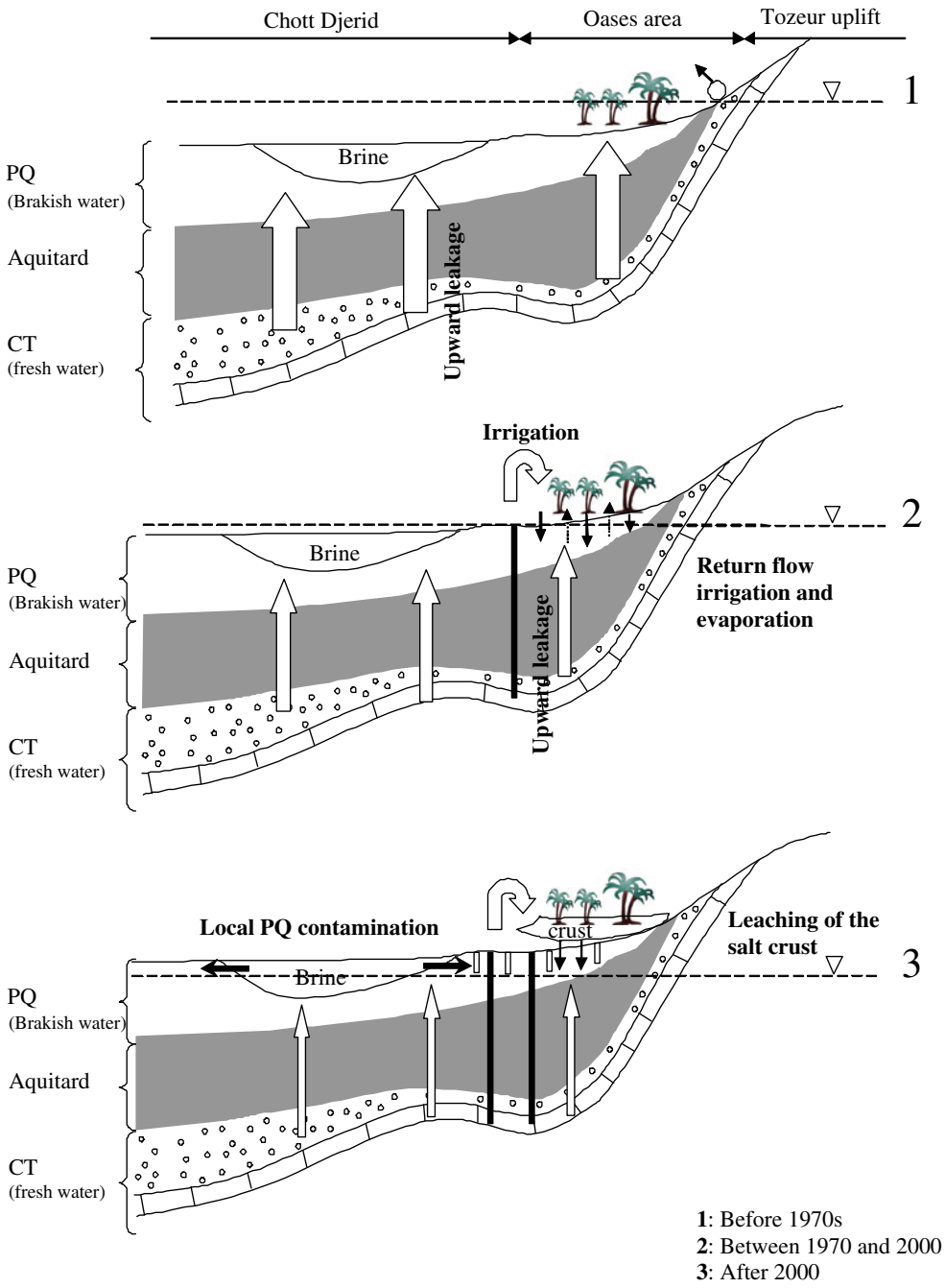

Fig. 13 Conceptual model of the CT potentiometric decline and its impact on the PQ water quality

irrigation contributes to formation of perched local 'oasis type aquifer 'mainly in oases areas, where salts concentrate and form crust (stage 2, Fig. 13).

Stage 3 summarises the current mechanism of the PQ water mineralisation by dissolution of salt crust. The decline of the water table PQ aquifer permits an eventual brine Chott invasion.

Indeed, local signs of PQ water table were recorded in the oases surrounding Chott El Gharsa, with predominance of NaCl, but are limited in time and across all areas of oases.

The combination of both hydrochemical and environmental isotope methods for the study of the PQ water table aquifer has provide basic information about its origins and mineralisation processes. The geochemical evolution of groundwater from the oases towards the Chotts margin is marked by increase of evaporitic salt leaching and highlighted by the correlations between the minerals part of these salts.

Control measures to limit contamination should include efforts to minimise the contamination risk from the sources discussed above, legal regulation and an increase in the irrigation efficiency as well as the implementation of effective drainage measures should go hand in hand with a strategy of moderation (Zamouri et al. 2007).

References

Adams S, Titus R, Pietersen K, Tredoux G, Harris C (2001) Hydrochemical characteristics of aquifers near Sutherland in the Western Karoo, South Africa. J Hydrol 241:91–103

Bryant RG (1999) Application of AVHRR to monitoring a climatically sensitive playa. Case study: Chott el Djerid, Southern Tunisia. Earth Surface Process Landf 24:283–302

Bryant RG, Sellwood BW, Millington AC, Drake NA (1994) Marine-like potash evaporate formation on a continental playa: case study Chott El Djerid, southern Tunisia. Sediment Geol 92:1–23

Bureau P, Roederer P (1960) Contribution à l'étude des sols gypseux du sud Tunisien. Croutes et encroutements gypseux de la partie sud du golfe de Gabès. Section spéciale d'études de pédologie et d'hydrologie. HAR Tunisia. 1–38

Castany G (1982) Bassin sédimentaire du Sahara septentrional (Algérie-Tunisie)—Aquifères du Continental intercalaire et du Complexe Terminal. Bulletin Bureau Recherches Géologiques Minières (BRGM). Série 2 3:127–147

Chadha DK (1999) A new diagram for geochemical classification of natural waters and interpretation of chemical data. J Hydrology 7:431–439

Coque R (1962) La Tunisie présaharienne: étude géomorphologique. Armond Colin, Paris

Drake NA, Bryant RG (1994) 'Monitoring the flooding ratios of Tunisian playas using AVHRR data. In: Millington AC, Pye K (eds) Climatic change in drylands. Wiley, London, pp 87–96

Drake NA, Bryant RG, Millington AC, Townshend JRG (1994) Playa geomorphology and sedimentology: mixture modelling applied to Landsat Thematic Mapper data of the Chott el Djerid, Tunisia. In: Renaut RW and Last WM (eds) The sedimentology and geochemistry of modern and ancient saline lakes, SEPM SP 50, Tulsa 123–135

Edmunds WM, Shand P, Guendouz AH, Moula A, Mamou A, Zouari K (1997) Recharge characteristics and groundwater quality of the grand Erg oriental basin. Tech. Rep. Wd/97/46R, Vienna

Edmunds WM, Guendouz AH, Mamou A, Moula A, Shand P, Zouari K (2003) Groundwater evolution in the Continental Intercalaire aquifer of southern Algeria and Tunisia: trace element and isotopic indicators. Appl Geochem 18:805–822

Epstein S, Mayeda TK (1953) Variations of ^{18}O content of waters from natural sources. Geochim Cosmochim Acta 4:213–224

Fontes JC, Edmunds WM (1989) The use of environmental isotope techniques in arid zone hydrology-—a critical review. UNESCO. IHP-III Project 5.2. Paris

Garcia MG, Del Hidalgo M, Blesa MA (2001) Geochemistry of groundwater in the alluvial plain of ucuman province Argentina. J Hydrology 9:597–610

Gautier M (1953) Les chotts, machines évaporitives complexes. Centre National de la Recherche Scientifique (CNRS). Colloques Internationaux 35:317–325

Gueddari M, Monnin C, Perret D, Fritz B, Tardy Y (1983) Geochemistry of brines of the Chott el Jerid in southern Tunisia—application of Pitzer's equations. Chem Geol 39:165–178

Guendouz A, Moulla AS, Remini B, Michelot JL (2006) Hydrochemical and isotopic behaviour of a Saharan phreatic aquifer suffering severe natural and anthropic constraints (case of Oued-Souf region, Algeria). J Hydrol 14:955–968

Hammi H, Musso J, M'nif A, Rokbani R (2003) Tunisian salt lakes evaporation studied by the DPAO method based on solubility phase diagrams. Desal 158:215–220

Hanshaw BB, Back W (1979) Major geochemical processes in the evolution of carbonate aquifer systems. J Hydrol 43:287–312

Henchiri M, Slim-S'Himi N (2006) Silification of sulphate evaporates and their carbonate replacements in Eocene marine sediments, Tunisia: two diagenetic trends. Sedimentology 53:1135–1159

Kamel S (2007) Caractérisation hydrodynamique et géochimique des aquifères du Djérid (Sud Tunisien). Thèse Doctorat. Univ. de Tunis

Kamel S (2011) Recharge of the plio-quaternary water table aquifer in Tunisian chotts region estimated from stable isotopes. Environ Earth Sci 63:189–199

Kamel S, Dassi L, Zouari K, Abidi B (2005) Geochemical and isotopic investigation of the aquifer system in the Djerid-Nefzaoua basin, southern Tunisia. Environ Geol 49:159–170

Kamel S, Younes H, Chkir N, Zouari K (2007) The hydro geochemical characterization of ground waters in Tunisian Chott's region. Environ Geol 54:843–854

Mamou A (1989) Caractéristiques et évaluation et gestion des ressources en eau du Sud tunisien. Thèse Doctorat. Univ. de Paris Sud. France

Mamou A, Kassah A (2002) Eau et développement dans le sud tunisien. Cahier du CERES, Série Géographique no. 23. Tunis 268p

Marfiaa AM, Krishnamurthya RV, Attekwnab EA, Pantonc WF (2004) Isotopic and geochemical evolution of groun and surface waters in a karst dominated geological setting: a case study from Belize Central America. Appl Geochem 19:937–946

Mc Intosh JC, Walter LM (2006) Paleowaters in Silurian–Devonian carbonate aquifers: geochemical evolution of groundwater in the Great Lakes region since the Late Pleistocene. Geochim Acta 70:2454–2479

Mc Lean W, Jankowski J, Lavitt N (2000) Groundwater quality and sunstainability in an alluvial aquifer. Australia. In: Sielilo et al (eds) Groundwater, past achievement and future challenges. Balkema, Rotterdam, pp 567–573

Millington AC, Drake NA, Townshend JRG, Quarmby NA, Settle JJ, Reading AJ (1989) Monitoring salt playa dynamics using Thematic Mapper data. IEEE Trans Geosci Remote Sens 27:754–761

ONM (Office National de la Météorologie : monthly bulletins of climatological records in Tunisia of 1950 to 2010). Tozeur and Nefta Meteorological Stations. Tunisia

OSS (2003) Système aquifère du Sahara septentrional. Observatoire du Sahara et du Sahel. UNESCO. Tech. Rep. 9973-856, Tunis

Plummer LN, Truesdell AH, Jones BF (1979) WATEQF, a Fortran IV version of WATEQ, a computer program for calculation chemical equilibrium of waters. US Geol. Survey Report WRI 76/13

Pouget M (1968) Contribution à l'étude des croûtes et encroûtements gypseux de nappe dans le sud Tunisien. Cah ORSTOM, Ser. Pedol 4:311–365

Schulz E, Abichou A, Chkir N, Hachicha T, Pomel S, Salzman U, Zouari K (2002) Sebkhas as ecological archives and the vegetation and landscope history of southeastern Tunisia during the last two millennia. J Afr Earth Sci 34:223–229

Shaw PA, Thomas DSG (1997) Pans, playas and salt lakes. In: Thomas DSG (ed) Arid zone geomorphology: process, form and change in drylands. Wiley, New York, pp 293–312

Swzey CS (2003) The role of climate in the creation and destruction of continental stratigraphic records: an example from the northern margin of the sahara desert. Climate controls on stratigraphy. SEPM Spec Publ 77:207–225

UNESCO (1972) Etude des ressources en eau du Sahara Septentrional. Projet ERESS. Nappe du Complxe Terminal Tech Rep 6:44

Zamouri M, Siegfried T, El Fahem T, Kriaa S, Kinzelbach W (2007) Salinization of groundwater in the Nefzawa oases region, Tunisia: results of a regional-scale hydrogeologic approach. Hydrogel J 15:1357–1375

Zouari K, Chkir N, Ouda B (2003) Palaeoclimatic variation in Maknassi basin (central Tunisia) during Holocene period using pluridisplinary approaches. IAEA, Vienna, CN 80-28

Zouari K, Kamel S, Chkir N (2006) Long term dynamic isotope and hydrochemical changes in the deep aquifer of Complex Terminal (Southern Tunisia). IAEA-TECDOC 507:127–156